



## Hyaluronan-coated nanoparticles: The influence of the molecular weight on CD44-hyaluronan interactions and on the immune response

Shoshy Mizrahy<sup>a,b,1</sup>, Sabina Rebe Raz<sup>c,1</sup>, Martin Hasgaard<sup>d</sup>, Hong Liu<sup>c</sup>, Neta Soffer-Tsur<sup>a,b</sup>, Keren Cohen<sup>a,b</sup>, Ram Dvash<sup>a,b</sup>, Dalit Landsman-Milo<sup>a,b</sup>, Maria G.E.G. Bremer<sup>c</sup>, S. Moein Moghimi<sup>d</sup>, Dan Peer<sup>a,b,\*</sup>

<sup>a</sup> Laboratory of Nanomedicine, Dept. of Cell Research and Immunology, Georg S. Wise Faculty of Life Science, Tel Aviv University, Tel Aviv, 69978, Israel

<sup>b</sup> Center for Nanoscience and Nanotechnology, Tel Aviv University, Tel Aviv, 69978, Israel

<sup>c</sup> RIKILT, Wageningen University and Research centre, P.O. Box 230, 6700 AE Wageningen, The Netherlands

<sup>d</sup> Centre for Pharmaceutical Nanotechnology and Nanotoxicology, Department of Pharmaceutics and Analytical Chemistry, University of Copenhagen, Universitetsparken 2, DK-2100 Copenhagen O, Denmark

### ARTICLE INFO

#### Article history:

Received 9 April 2011

Accepted 18 June 2011

Available online 2 July 2011

#### Keywords:

Hyaluronan  
Nanoparticles  
CD44

Complement activation  
Nanomedicine

### ABSTRACT

Hyaluronan (HA), a naturally occurring glycosaminoglycan, exerts different biological functions depending on its molecular weight ranging from 4000–10M Da. While high Mw HA (HMw-HA) is considered as anti-inflammatory, low Mw HA (LMw-HA) has been reported to activate an innate immune response. In addition, opposing effects on cell proliferation mediated by the HA receptor CD44, have also been reported for high and low Mw HA. We have previously demonstrated that HMw-HA can be covalently attached to the surface of lipid nanoparticles (NPs), endowing the carriers with long circulation and active targeting towards HA-receptors (CD44 and CD168) highly expressed on tumors. Here we present a small library of HA-coated NPs distinguished only by the Mw of their surface anchored HA ranging from 6.4 kDa to 1500 kDa. All types of NPs exerted no effect on macrophages, T cells and ovarian cancer cells proliferation. In addition, no induction of cytokines or complement activation was observed. The affinity towards the CD44 receptor was found to be solely controlled by the Mw of the NPs surface-bound HA, from extremely low binding for LMw-HA to binding with high affinity for HMw-HA. These findings have major implications for the use of HA in nanomedicine as LMw-HA surface modified-NPs could be a viable option for the replacement of polyethylene glycol (PEG) when passive delivery is required, lacking adverse effects such as complement activation and cytokine induction, while HMw-HA-coated NPs could be used for active targeting to CD44 overexpressing tumors and aberrantly activated leukocytes in inflammation.

© 2011 Elsevier B.V. All rights reserved.

### 1. Introduction

Hyaluronan (HA) is a linear high Mw glycosaminoglycan (GAG) composed of alternating disaccharide units of D-glucuronic acid and N-acetyl-D-glucosamine with  $\beta$ -[1,4] interglycosidic linkage [1]. HA possesses outstanding hydrodynamic properties especially regarding to its viscosity and ability to retain water [2]. HA is an important joint lubricant and an organ structural stability material [2]. In addition, HA is essential for proper cell growth, embryonic development, healing processes, inflammation, and tumor development [2,3].

High Mw (HMw) HA possesses several advantages, which make it an attractive targeting moiety decorating drug delivery vehicles: it is water

soluble, biodegradable, and suggested to be biocompatible, non-toxic, non-immunogenic and can be chemically modified [4,5]. We and others have demonstrated that LMw-HA [6,7] (with higher HA density that can improve binding avidity) or HMw-HA [8–11], can be covalently attached to the surface of lipid nanoparticles (NPs) [3,6,7,9–12] or polymersomes [13,14] and efficiently target epithelial cancer cells and leukocytes expressing HA receptors. The HA coating endows the carriers with active targeting towards HA receptors (CD44 and CD168) highly expressed on various tumors such as squamous cell carcinoma, ovarian, colon, stomach, glioma, and many types of leukemia, lymphoma and myeloma [3,12,15–18].

HA exerts different biological functions depending on its molecular weight ranging from 4000–10 MDa. HMw HA is considered as anti-angiogenic and non-immunogenic, whereas low Mw (LMw) HA is regarded as inflammatory, immuno-stimulatory and angiogenic [19]. Nevertheless, not all literature reports are consistent, revealing a more complex behavior. For example, administration of LMw HA to tumor xenografts of various types inhibits rather than stimulates tumor

\* Corresponding author at: Laboratory of Nanomedicine, Department of Cell Research and Immunology, Tel Aviv University, Tel Aviv 69978, Israel. Tel.: +972 3640 7925; fax: +972 3640 5926.

E-mail address: [peer@post.tau.ac.il](mailto:peer@post.tau.ac.il) (D. Peer).

<sup>1</sup> SM and SRR contributed equally to this work.

growth and overexpression of hyaluronidase suppresses colon and breast carcinoma growth in xenografts [2].

Here we report on the preparation and characterization of a small library of lipid-based nanoparticles distinguished by the length of their surface-anchored HA ranging from 6.4 kDa to 1500 kDa. The effect of HA Mw on HA-CD44 interactions, cell proliferation, cytokine induction and complement activation in human serum was tested.

## 2. Materials and methods

### 2.1. Materials

Pure Soybean phosphatidylcholine (Phospholipon 90 G) was a kind gift from Phospholipid GMBH (Germany). 1,2-dipalmitoyl-sn-glycero-3-phosphoethanolamine (DPPE) and Cholesterol (Chol) were purchased from Avanti Polar Lipids Inc. (Alabaster, AL, USA). Sodium hyaluronate with average Mw of 6.4 kDa, 31 kDa, 132 kDa, 700 kDa and 1500 kDa were purchased from Lifecore Biomedical, LLC (MN, USA). Ethyl-dimethyl-aminopropyl-carbodiimide (EDC) and trypan blue were purchased from Sigma-Aldrich Co. (St. Louis, MO, USA). Biacore CM5 sensor chip and amine coupling kit containing *N*-hydroxysuccinimide (NHS) and EDC were purchased from GE Healthcare (Uppsala, Sweden). Alexa Fluor 488 Rat anti-human CD44 and IgG2b isotype control were purchased from BioLegend (San Diego, USA). CD44-Fc, TNF- $\alpha$  and IL-10 ELISA kits were purchased from R&D systems (Minneapolis, MN, USA). C5a and SC5b-9 ELISA kits were purchased from Quidel Cop. (San Diego, CA, USA). Materials for cell cultures, Cell Proliferation Kit (XTT) and EZ-PCR Mycoplasma Test Kit were purchased from Biological Industries Co. (Beit Haemek, Israel). All other reagents were of analytical grade.

### 2.2. Methods

#### 2.2.1. Preparation of NPs

Multilamellar vesicles (MLV) composed of PC:Chol:DPPE at mole ratios of 15:4:1, were prepared by the traditional lipid-film method [10,11,20,21]. Briefly, the lipids were dissolved in ethanol, evaporated to dryness under reduced pressure in a rotary evaporator (Buchi Rotary Evaporator Vacuum System Flawil, Switzerland) and hydrated by the swelling solution that consisted of buffer alone (PBS) at pH 7.4. This was followed by extensive agitation using a vortex device and a 2 h incubation in a shaker bath at 37 °C. The MLV were extruded through a Lipex extrusion device (Northen lipids, Vancouver, Canada), operated at 65 °C and under nitrogen pressures of 200–500 psi. The extrusion was carried out in stages using progressively smaller pore-size polycarbonate membranes (Whatman Inc, UK), with several cycles per pore-size, to achieve unilamellar vesicles in a final size range of ~100 nm in diameter. Lipid mass was quantified as previously reported [11].

#### 2.2.2. Surface modification of NPs

The surface modification was carried out on the NPs, according to our previously reported procedures [10,11,21]. A small library consisting of five different types of targeted and stabilized NPs (tsNPs) was prepared by surface modification of pre-formed NPs with different molecular weights of HA. The average Mws of the surface anchored HA were 6.4 kDa, 31 kDa, 132 kDa, 700 kDa and 1500 kDa. Briefly, HA was dissolved in 0.1 M sodium acetate buffer pH 4.5 to a final concentration of 2 mg/ml and preactivated by incubation with EDC, for 2 h at 37 °C. At the end of this step, the activated HA was added to a suspension of the drug-free NPs, buffering by 0.1 M borate buffer pH 9 and incubated overnight at 37 °C. At the end of the incubation, the resulting tsNPs were separated from excess reagents and by-products by centrifugation ( $1.3 \times 10^5$  g, 4 °C, 40 min) and repeated washings with PBS, adjusting the pH back to physiological one. A batch of NPs underwent the same processes, except that

sodium acetate buffer at pH 4.5 was added instead of the activated HA. HA was quantified as previously reported [11].

#### 2.2.3. Particle size distribution and zeta potential measurements

Particle size distribution and zeta potential measurements were determined by light scattering using Malvern nano ZS Zetasizer (Malvern Instruments Ltd. Worcestershire, UK). Size measurements were performed in PBS pH 7.4 and zeta potential measurements were performed in 0.05XPBS pH 7.4. Each experimental result was an average of at least six independent measurements. NPs had a mean diameter of  $113 \pm 18$  nm, whereas the addition of HA of various sizes increased the mean diameter to about  $140 \pm 15$  nm for tsNPs 6.4 kDa, 31 kDa, 132 kDa, 700 kDa and 1500 kDa, respectively. NPs had a zeta potential of  $-9.5 \pm 3.9$  mV, whereas the addition of the HA coating decrease the zeta potential to about  $-32 \pm 5$  mV for tsNPs 6.4, 31, 132, 700, 1500 kDa, respectively.

#### 2.2.4. Surface plasmon resonance study of Interaction of free HA and tsNPs with CD44

Recombinant human CD44-Fc chimera was immobilized on a 100 nm-thick carboxymethylated dextran sensor chip (CM5) using a common amine coupling chemistry in Biacore 3000 [22]. Briefly, the sensor chip surface was activated with 1:4 mixture of *N*-hydroxysuccinimide (NHS) and ethyl-3(3-dimethylamino)propyl carbodiimide (EDC) for 7 min. CD44-Fc was dissolved in 10 mM acetate buffer pH 4 to a concentration of 17  $\mu$ g/mL and flown over the activated surface for 5 min. The remaining reactive groups were blocked with 1 M ethanolamine pH 8.5. For reference, additional blank flow channel (FC) was prepared by EDC/NHS activation but without introducing the receptor to the surface. Throughout all the SPR measurements 10 mM sodium phosphate pH 7 supplemented with 150 mM NaCl was used as the running buffer.

**2.2.4.1. Kinetic analysis of HA-CD44 interaction.** For collection of kinetic data, a series of HA concentrations (from 0.032 nM to 10  $\mu$ M) were injected at 50  $\mu$ L/min over the CD44-Fc coated FC and blank FC at 20 °C. For each size of HA an individual optimal concentration range was selected according to obtained sensorgrams. For double referencing, buffer blank injections were periodically performed in each run. After each measurement cycle the sensor chip surface was regenerated with 10 mM NaOH for 30 s. The association and dissociation were monitored for 360 and 640 s respectively. Obtained sensorgrams were double referenced to blank FC and buffer injections in order to correct for bulk refractive index changes and experimental artifacts respectively [23]. Further on, the sensorgrams were zeroed, aligned, cropped (to exclude the regeneration), corrected for spikes and uploaded to ClampXP Biosensor Analysis Software (version 3.50) which combines numerical integration and nonlinear global curve fitting routines [24]. The kinetic analysis of HA-CD44 interaction was obtained by fitting the collected data to "heterogeneity model" with 2–4 independent binding sites.

**2.2.4.2. Interaction of tsNPs with CD44.** tsNPs coated with different sizes of HA (6.4, 31, 132, 700 and 1500 kDa) were diluted with 50 mM sodium phosphate buffer pH 7.0 with 150 mM sodium chloride to a concentration of 1 mg/ml, which was found to be a good compromise between sufficient binding response and bulk refractive index shift. The tsNPs were injected over the sensor chip surface coated with CD44-Fc (600 RU immobilization level) at 3  $\mu$ L/min for 1200 s. The dissociation in the running buffer took place for another 1200 s. Between the measurement cycles the sensor chip surface was regenerated with 10 mM NaOH at a flow rate of 200  $\mu$ L/min. The responses on the blank FC were subtracted from the CD44-Fc coated FC. Additionally, the responses obtained with NPs not coated with HA were subtracted from the responses obtained with the HA-coated NPs

to compensate for the bulk shift. No binding was observed between the non-coated NP and CD44-Fc.

### 2.2.5. Cell culture growth and maintenance

Monolayers of NCI/ADR-RES (human ovarian adenocarcinoma Adriamycin resistant) and RAW 264.7 (mouse Macrophages) cells were grown in 100 × 20 mm dishes. TK-1 (mouse T cell lymphoma) cells were grown in suspension. RAW264.7 cells were cultured in Dulbecco's modified Eagle's medium (DMEM). TK-1 and NCI/ADR-RES cells were cultured in RPMI-1640 medium as previously reported [11,25]. All growth media contained 10% fetal bovine serum, Penicillin (100 U/ml), Streptomycin (0.1 mg/ml), Nystatin (12.5 U/ml) and L-glutamine (2 mM). Cells were free of Mycoplasma contamination as determined by a Mycoplasma PCR test carried out every 3 months. Viability of cultures used in the experiments was >90%, as determined by the trypan blue method.

### 2.2.6. Flow cytometry analysis of surface CD44

Flow cytometry of cell surface CD44 antigens was performed as previously described [11,12]. The following mAbs were used: Alexa Fluor 488 Rat anti-human CD44 and IgG2b isotype control. Data were acquired on FACScan with CellQuest software (Becton Dickinson, Franklin Lakes, NJ). Data analysis was performed using FlowJo software (Tree Star, Inc. Oregon, USA).

### 2.2.7. Cell proliferation assay

Twenty-four hours prior to an experiment, cells of the desired line were seeded onto 96-well multiwell culture plates at densities in the range of  $4\text{--}9 \times 10^3$  cells/mL. The experiments were initiated on sub-confluent monolayers. TK-1 cells were treated in suspension. The cells were incubated (see growth conditions in Section 2.2.6) with the selected treatment media containing NPs or tsNPs for 4 h and 24 h, at the end of which the media was removed and the cells washed and fed with serum-supplemented growth media. The experiment was terminated 72 h later and proliferation was determined for each well by the XTT cell proliferation kit.

### 2.2.8. Cytokine induction assay

RAW264.7 cells were seeded 48 h prior to the experiment in 96-well multiwell culture plates at a density of  $1 \times 10^5$  cells per well, in culture medium supplemented with 5% FBS. The cells were incubated with the selected treatment media containing NPs or tsNPs (250 µg/ml) for 6 h. Cell stimulation with LPS (10–100 ng/ml) was used as positive control. The levels of TNF-α and IL-10 secreted to the medium were measured by ELISA.

### 2.2.9. Serum characterization and assays of in vitro human complement activation

Procedures for preparation of fresh human serum and validation assessment of serum functional activity of classical, lectin and the alternative pathways of complement were done as previously reported [26]. Only sera with all three functional complement pathways were used for subsequent studies. To measure complement activation in vitro, we determined NPs-induced rise of human serum complement activation products C5a and SC5b-9 using respective ELISA kits as described in detail previously [27,28]. For measurement of complement activation, the reaction was started by adding NPs (5 mg total lipid/mL serum final concentration) to undiluted fresh human serum (typical NPs/serum volume, 1:4) in Eppendorf tubes (in triplicate) in a shaking water bath at 37 °C for 30 min. Reactions were terminated by the addition of PBS supplemented with 25 mM EDTA. Control serum incubations contained saline (the same volume as the NPs) for assessing background levels of complement activation products. Zymosan was suspended in sterile saline and used as an established positive control for monitoring complement activation at a final concentration of 1 mg/mL serum. In all experiments pH was

maintained between 6.8 and 7.1. The efficacy of NPs treatment was established by comparison with baseline levels using paired *t*-test.

### 2.2.10. Statistical analysis

All statistical analyses were done using GraphPad Prism® 5 software (San Diego, CA, USA). Results are expressed as mean ± SD. Differences between two means were tested using an unpaired, two-sided Student's *t*-test. Differences between treatment groups were evaluated by one-way ANOVA with significance determined by Bonferroni adjusted *t*-tests.

## 3. Results and discussion

### 3.1. The effect of HA Mw on the interaction of HA with the CD44 receptor using SPR analysis

The effect of HA Mw on HA-CD44 interaction was determined using Surface Plasmon resonance (SPR). Human recombinant CD44-Fc (~170 kDa) was immobilized on 100 nm thick carboxymethylated dextran (CM-dextran) sensor chip using common amine coupling chemistry (EDC/NHS). The three dimensional CM-dextran matrix offers several advantages such as a hydrophilic setting for molecular interaction and the preservation of the mobility of the immobilized CD44, enabling improve kinetic characterization [29]. When performing kinetic experiments, low sensor surface capacity is desired [23], however to compare between different sizes of HA the responses with the lowest Mw should be still detectable. We initially tested different immobilization levels of CD44-Fc with HA with an average Mw of 132 kDa and 6.4 kDa and found that a minimal surface immobilization level of approximately 900 RU is needed to obtain robust responses (data not shown). Five Mw ranges of free HA were studied in order to investigate how the Mw of HA affects binding to CD44. The average Mw of the HA tested were: 6.4, 31, 132, 700 and 1500 kDa. Each HA in concentration range from 0.032 nM to 10 µM was injected over the FC with the immobilized CD44-Fc (850 RU immobilization level). For each HA size an optimal concentration range was chosen according to the obtained sensorgrams (Fig. 1). In order to estimate the availability of the binding partners of CD44 and of HA, the stoichiometry of the binding interaction was calculated for each HA size as follows. Given the expected molecular weight of CD44-Fc (170 kDa) in a dimer form and  $1 \text{ RU} = 1 \text{ pg/mm}^2$  protein relationship [30] we estimated surface density of ~3 receptors per 1000 nm<sup>2</sup>. In aqueous solutions flexible HA forms a random coil [2]. Based on the Mw, the gyration radius of the folded HA can be determined through the following equation:  $R_g = 1.3 \text{ nm} \times (\text{Mw (kDa)})^{0.6}$  [31].

Assuming homogenous receptor distribution on the sensor chip surface, the number of CD44 molecules that can interact with a single HA molecule was calculated (Table 1).

The calculation results showed that for Mw of 132 kDa and higher each HA molecule interacted with multiple receptors on the sensor surface. Given each CD44-Fc dimer has 4 binding sites and that each high Mw HA can be bound by multiple receptors the kinetic data of such interaction is too complex to be fitted with the commonly applied 1:1 interaction model as was previously attempted [32]. The kinetic model, which gave the best fit to the data obtained in this study, was the "heterogeneity model" with two independent binding sites for 6.4 kDa HA and with 4 independent binding sites for the rest of the HAs. With the exception of the HA6.4 kDa the data fitting was in good agreement with the expected 4 binding sites on each CD44-Fc dimer. HA6.4 kDa interaction data slightly deviated from the model at high concentrations. Adding or removing binding partners to the model did not improve the fitting. For HA700 kDa and HA1500 kDa the dissociation constant could not be resolved also with prolonged monitoring time (data not shown), most likely due to multiple binding sites on each HA and re-binding events during dissociation. Taking into account the complexity of the interaction and

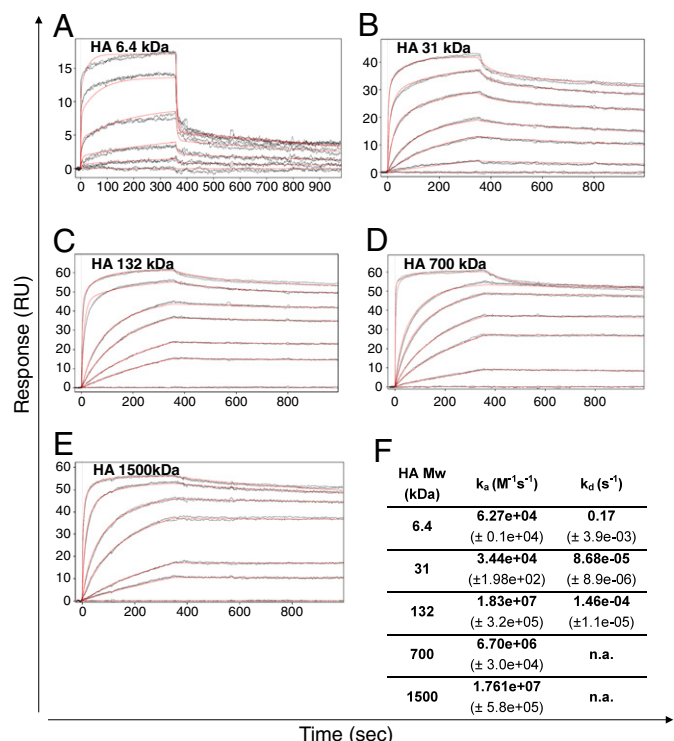


**Fig. 1.** SPR-based kinetic analysis of CD44 interaction with different HA sizes. Five size ranges of HA with average Mw of: 6.4 kDa (A), 31 kDa (B), 132 kDa (C), 700 kDa (D) 1500 kDa (E), were injected over the CD44-Fc coated sensor chip at 6 different concentrations: HA6.4 (0.1  $\mu$ M–10  $\mu$ M), HA31 (0.3nM–0.5  $\mu$ M), HA132 (0.2 nM–0.1  $\mu$ M), HA700 (0.03 nM–0.1  $\mu$ M) and HA1500 (0.2 nM–0.1  $\mu$ M). Following 360 s of interaction, the HA was replaced by the buffer and dissociation was monitored for 640 s. Representative sensorgrams of duplicate HA injections (black lines) were globally fitted to heterogenic interaction model with 4 binding sites (red lines) yielding association and dissociation constants ( $k_a$  and  $k_d$ ) (F).

experimental artifacts such as steric hindrance, crowding and aggregation we address the kinetic analysis results as trend indicators and not as absolute values. The results of the interaction data (black curves) and the kinetic model fit (red curves) are shown in Fig. 1 A–E. The kinetic constants derived from these data are summarized in Fig. 1F. As shown in Fig. 1, there is a clear increase in global affinity ( $K_D$ ) as a function of HA Mw starting from  $2.7 \mu M^{-1}$  for HA6.4 kDa and ending up with  $7.9 pM^{-1}$  for HA132kDa. There are two main changes in HA Mw in which a clear increase in the affinity is noticed: from HA 6.4 kDa to HA31kDa and from HA31 kDa to HA132 kDa. Above HA132 kDa the increase in binding affinity is not significant however as mentioned, there is a difference in dissociation. In addition, the reversibility of HA binding is also strongly dependent on the Mw of HA. While a high dissociation rate is noticed for HA 6.4 kDa, essentially no dissociation is noticed above HA 700 kDa (Fig. 1A and E). The differences in  $K_D$  between HA with an average Mw of 6.4 kDa to 31 kDa have been previously reported [33] and are characterized by a significant decrease in dissociation. This can be attributed to the increase in the avidity as a result of multivalent interactions.

**Table 1**  
Estimated CD44-Fc coverage by free HA at different MWs.

HA Mw (kDa)	Radius of gyration (nm)	Area (nm <sup>2</sup> )	CD44 coverage (CD44 molecules available per HA)
6.4	4	49	1 (0.16)
31	10	327	1
132	24	1709	5–6
700	66	13,678	44
1500	105	34,365	110

The  $K_D$  values received in this study differ from the ones obtained from binding fluorescently labeled HA to CD44 expressing cell, which are in the  $\mu$ M range [33] but with good agreement with  $K_D$  values obtained from measurements performed with radio-labeled HA [34]. When comparing SPR analysis to experiments performed on CD44 expressing cells one should keep in mind that there are several differences. At first, the Fc fusion protein differs from the dimers formed on cell surface. In addition, the surface density reported here is up to 12 fold higher than the average surface density reported for cell surfaces [31,35,36]. Although it should be noted that the receptor distribution on cell surfaces is not homogenous and that specific areas of high receptor concentration exist [31]. Therefore, a more accurate calculation of  $K_D$  performed on cells would be obtained not by relating to the average receptor density but rather to the local and temporal receptor density. When comparing the  $K_D$  obtained in this study to values derived from previously reported SPR analyses, several fold differences are observed. This is probably due to the fact that the previous SPR studies extracted the values from equilibrium analysis, often using sensorgrams, which failed to reach equilibrium [37]. Moreover, previously reported SPR data were obtained from highly loaded sensor surfaces [32,37,38], complicating the analysis further and misrepresenting the interaction between HA and CD44.

**3.2. The effect of HA Mw on the interaction of tsNPs with the CD44 receptor using SPR analysis**

A small library of NPs and tsNPs distinguished by the Mw of their surface-anchored HA was prepared. Neutral in charge phospholipids have been used to prepare nano-scale liposomes (~100 nm). In the case of the tsNPs, HA was attached to the outer surface of the liposomes, through covalent linkage to dipalmitoylphosphatidylethanolamine (DPPE) as detailed in the experimental section.

The estimation of the effect of NPs surface bound HA Mw on the interaction with CD44 was also performed using SPR analysis. The experimental conditions were different from those used for kinetic analysis in order to be able monitor the receptor interaction with the NPs. tsNPs coated with HA6.4 kDa, HA31 kDa, HA132 kDa, HA700 kDa and HA1500 kDa were diluted with 50 mM sodium phosphate buffer pH 7.0 with 150 mM sodium chloride to a concentration of 1 mg/ml, which was found to be a good compromise between low bulk responses and sufficient robust signal. The tsNPs were injected over the sensor chip surface coated with CD44-Fc at 3  $\mu$ L/min for 1200 s. The dissociation of tsNPs from CD44 was monitored for additional 1200 s. No binding was observed between the uncoated NPs and CD44-Fc. The results show same trend as was observed in the experiments with free HA, clearly indicating stronger binding of HMW HA to the receptor (Figs. 1 and 2). However some differences were observed for tsNPs 132 kDa and tsNPs 31 kDa. tsNPs 132 kDa showed lower binding than tsNPs 700 kDa and 1500 kDa whereas free HA binding for 132 kDa was very similar to HA700 kDa and 1500 kDa. tsNPs 31 kDa showed lower binding in comparison to the free HA (Fig. 1B). Low response of the 6.4 kDa -tsNPs was as expected and with a good agreement to the low binding affinity observed with the free 6.4 kDa HA. Lower binding responses of 31 kDa – and 132 kDa – tsNPs could be explained by the decrease in the degree of freedom of the HA molecule when bound to the particles' surface. Some potential reactive sites might bind to the particles' surface and become unavailable for CD44 receptor binding. In addition, the dissociation of HA 700 kDa and 1500 kDa appeared very similar to that of HA132 kDa and this can account for the rebinding of tsNPs 132 kDa to the receptor during the dissociation. Since the SPR responses are based on the refractive index change, the binding of differently sized free HA cannot be compared directly due to different molecular weights. Therefore, the interaction of different Mws of free HA with CD44 is better described based on the affinity constants and not based on the direct comparison of the obtained signal at the same

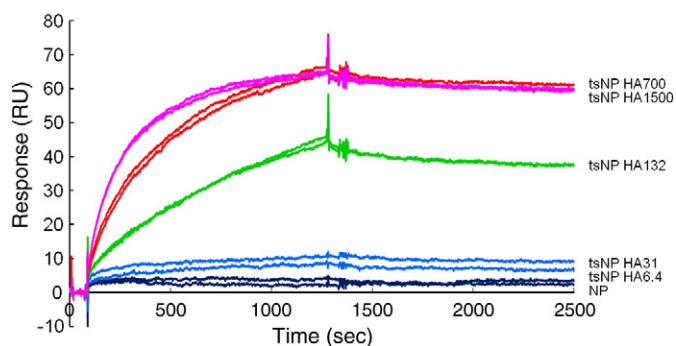


**Fig. 2.** tsNPs–CD44 interaction studied by SPR. Representative sensorgrams of tsNPs–CD44 interaction monitored by SPR are presented. tsNPs coated with HA of an average Mw of 6.4 kDa, 31 kDa, 132 kDa, 700 kDa and 1500 kDa and non-coated NPs at a concentration of 1 mg/ml were injected in duplicate over CD44-Fc coated sensor surface. The interaction was monitored for 1200 s, followed by dissociation in buffer for another 1200 s. The sensorgrams were double referenced and normalized to the bulk shift caused by the non-coated NPs.

concentration. Nevertheless, the signals obtained with HA-coated NPs can be directly compared, because the main bulk shift is produced by the NPs themselves.

### 3.3. The effect of NPs and tsNPs on cell proliferation

High Mw HA (HMw-HA) and low Mw HA (LMw-HA) where reported to have opposing effects on cell proliferation through CD44 [39–41], which appear to be strictly regulated by signaling pathways [41]. While binding of HMw-HA to CD44 suppresses cell cycle

progression, binding of LMw-HA stimulates it [40]. This is a result of a differential regulation of signaling pathways to cyclin D1, which is the common signaling target for both HMw and LMw HA. These opposing effects on cell proliferation have been shown for smooth muscle cells, fibroblasts and endothelial cells [39–42]. In melanoma cells, the opposing effects on cell proliferation were also shown however in this case, HMw-HA and not LMw-HA promoted cell proliferation [43].

We therefore investigated whether tsNPs with different surface anchored HA Mws would have an effect on cell cycle progression *in vitro*. Three cell lines were chosen for this purpose: NCI/ADR-RES (NAR), TK-1 and RAW 264.7. All cell lines tested were characterized with high CD44 expression (Fig. 3A). The cells were incubated in the presence of NPs and tsNPs as described under materials and methods, and cell proliferation was tested using the XTT assay (Fig. 3B). The NPs and tsNPs tested had no impact on cell proliferation. The tested tsNPs are therefore a viable option for drug delivery purposes. The possible contradiction with literature reports can be explained in several lines of evidence. The effects of HA Mw on cell proliferation seem to be cell-specific, and depending on the HA medium concentration. In addition, the ability of the HA molecule to internalize into specific cells is another important factor that determines signaling cascade (such as outside-in signaling) [39–42]. The lack of effect reported here can be attributed to differences in HA medium concentration, which are significantly lower for the tsNPs [10,11,39–41].

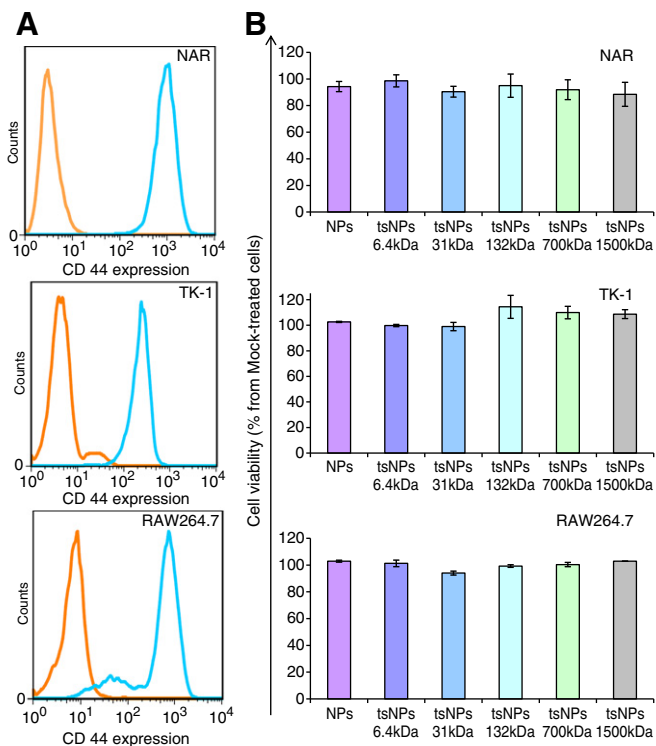


**Fig. 3.** The effect of NPs and tsNPs on cell viability of CD44-expressing cells. A. Representative histograms of CD44 expression in NAR, TK-1 and RAW 264.7 cells determined by flow cytometry. Orange line – isotype control; blue line – anti-pan CD44 antibody. B. The effect of NPs and tsNPs on the viability of NAR, TK-1 and Raw 264.7 cells. Data are expressed as the mean  $\pm$  SD obtained from XTT assay normalized against untreated cells.

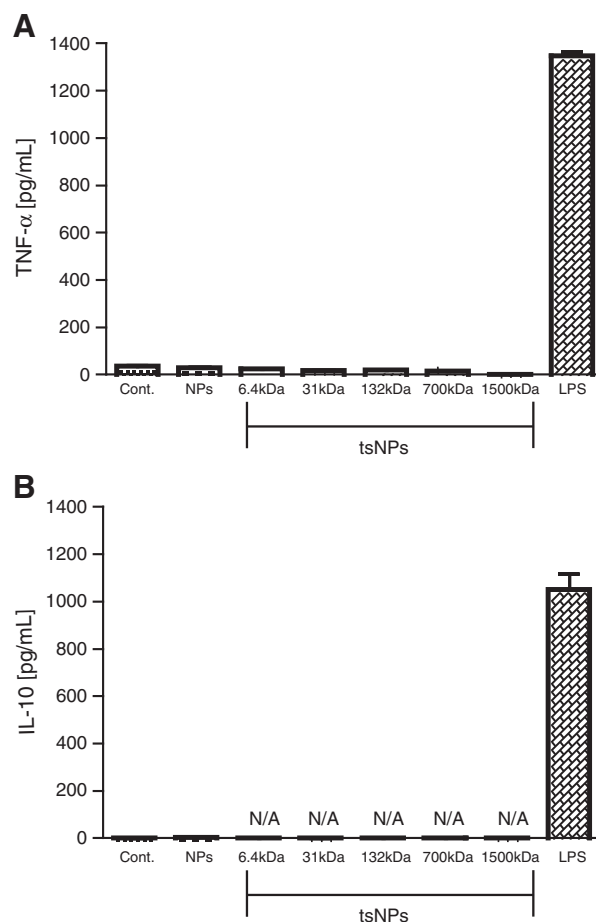


**Fig. 4.** Macrophage activation by NPs and tsNPs. Mouse Macrophage cells (RAW264.7) were incubated at 37 °C for 6 h with NPs and tsNPs at a concentration of 250  $\mu$ g/mL. LPS (100 ng/mL) served as a positive control. TNF- $\alpha$  and IL-10 release to the medium were measured by ELISA. Data are expressed as the mean  $\pm$  SD of at least three independent experiments. N/A – below detection level.

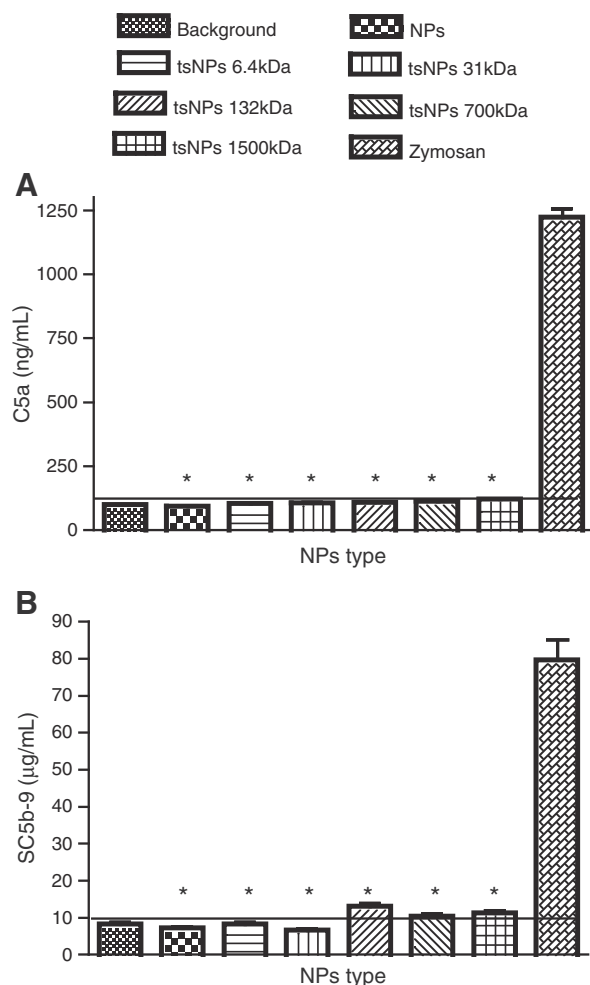


**Fig. 5.** The effect of NPs and tsNPs on complement activation. The levels of C5a and SC5b-9 were measured by ELISA. A. NPs and tsNPs-mediated elevation of complement activation products in human serum. The horizontal lines (A, B) denote background levels of activation products. A. Activation product C5a. B. Activation product SC5b-9. \* Denoted p values < 0.001 compare to a positive control, Zymosan.

#### 3.4. The effect of NPs and tsNPs on Macrophages activation

HMw-HA is known to play a homeostatic role [44]. However, upon tissue injury HMw-HA is broken down to LMw-HA, which has been reported to activate an innate immune response via Toll-Like Receptor (TLR) 2 and TLR4 [44,45]. Several studies demonstrated that LMw-HA possesses the ability to stimulate Macrophages recruited to sites of inflammation to produce important mediators of tissue injury and repair [46]. LMw-HA has been shown to induce cytokines (IL-8, IL-12, and TNF- $\alpha$ ), chemokines, reactive nitrogen species, and growth factors [44,46]. Nevertheless, literature reports regarding the effects of HA Mw on macrophage activation are not consistent: Wang et al. [47] has shown that relatively HMw HA (500–800 kDa) significantly stimulated the murine macrophage cell line RAW 264.7 to produce TNF- $\alpha$ . However, a recent study by Krejcová D. et al. [48] who tested the effect of a large range of HA Mws (11, 52, 87, 250 and 970 kDa) on macrophage activation reported that no molecular weight induced production of TNF- $\alpha$  in two murine macrophage cell lines: RAW 264.7 and MHS. Therefore, we tested whether tsNPs with different surface anchored HA Mws can induce macrophage activation. We first tested free HA. LMw HA tested (6.4 and 31 kDa) only gave a marginal increase (up to 50% in TNF- $\alpha$  release above the basal level), whereas in the larger fragments (>31 kDa) TNF- $\alpha$  release was as low as the basal level (data not shown). LPS, a potent macrophage activator that mediates acute inflammation [49,50], was used as positive control since as with short fragments of HA,

the initiated inflammatory responses is facilitated by Toll-like receptor (TLR)4 [45]. To this end, we monitored the levels of secreted TNF- $\alpha$  and IL-10 from Macrophages following incubation with NPs or tsNPs as described in the methods section. We chose to monitor the levels of TNF- $\alpha$  since it is the first cytokine to be released after activation of essentially all TLRs and is regarded as the key pro-inflammatory cytokine [20,51]. In addition, TNF- $\alpha$  also enhances the production of the key anti-inflammatory cytokine IL-10 [52], which in turn suppresses TNF- $\alpha$  to complete the negative regulatory feedback cycle. As shown in Fig. 4 no cytokine induction was observed regardless of the HA Mw anchored to the NPs' surface. These results are not in good agreement with previous studies in which free LMw-HA but not HMw-HA was shown to induce inflammatory gene expression in peritoneal and alveolar Macrophages [44,49]. However, this discrepancy is not unexpected as the amounts of HA used for Macrophage activation were significantly higher in comparison to the amount of HA immobilized on tsNPs' surface and cultured with the cells [10,11,44,49]. In addition, the HA on the tsNPs surface is covalently attached by a stable amide bond, which hinders processing by cells and may account for the lack of Macrophage activation.

#### 3.5. The effect of NPs and tsNPs on human complement activation

Activation of the complement system, as reported for (polyethylene glycol), PEG-grafted liposomes, may initiate adverse reactions among sensitive individuals and represents a potential barrier to the clinical use, since complement-mediated hypersensitivity reactions may contribute towards cardiac anaphylaxis [27,53]. Several studies suggested a key role for the anionic phosphate oxygen moiety of phospholipid-mPEG in activation of both classical and alternative pathways of the complement and anaphylatoxin production [27], and indeed methylation of the phosphate oxygen of phospholipid-mPEG conjugate, and hence the removal of the negative charge, prevented complement activation [27]. Since HA is a polyanion under physiological conditions, we examined whether tsNPs can trigger complement activation and whether specific HA Mws anchored to the surface of the NPs are more likely to induce complement activation. These experiments could further shed light on establishing the role of anionic charge and/or identification of structural architectures that incite complement activation. Accordingly, we added NPs and tsNPs to undiluted human serum and determined the levels of the terminal complement pathway activation markers C5a and SC5b-9 by ELISA as described under materials and methods. Under normal conditions, activation of all three established pathways of complement results in the formation of a C5 convertase multi-molecular enzyme capable of cleaving C5 to C5a and C5b. The 9 kDa C5a fragment is the most potent of all complement anaphylatoxins, where elevated levels of fluid phase and adsorbed C5a are usually associated with haemocompatibility of some biomaterials and particulate drug carriers [28]. C5b is a key constituent of the terminal complement complex leading to the assembly of membrane-attack complex C5b-9. In the fluid phase C5b-9 forms a complex with vitronectin or the S protein and the non-lytic SC5b-9 is an established marker of the terminal complement pathway and a measure of the activation of the whole complement cascade [27].

The results clearly demonstrate that tsNPs do not trigger complement activation in human serum, since both C5a and SC5b-9 levels remain comparable with their respective baseline values (Fig. 5). Complement activation, however, proceeded with zymosan (Fig. 5) as well as with PEG-grafted liposomes [27] of similar size ranges to tsNPs (DPPC:DPPG, mole ratio 9:10 and DPPC:mPEG2000-DPPE, mole ratio 9.5:0.5). For instance, with PEGylated liposomes, generated SC5b-9 levels were  $36 \pm 2.8 \mu\text{g/mL}$  serum. It should be emphasized that although the levels of complement activation are significantly higher for PEG-grafted liposomes in comparison to the tsNPs, the particle surface charge of tsNPs are much more negative

than PEGylated liposomes [54]. Therefore, the anionic charge per se is probably not the major reason for complement activation, but rather complement activation depends on the type of functional groups and overall architectural structure [55,56].

#### 4. Conclusions

We have presented a small library of lipid NPs distinguished only by the Mw of their surface anchored HA. All NPs, regardless of their surface-anchored HA Mw revealed no apparent effect cellular proliferation. In addition, no Macrophage activation or complement activation were detected. The affinity towards the HA receptor CD44 however, was shown to be controlled solely by adjusting the Mw of the NP surface HA, from weak binding for LMw-HA to binding with high affinity for HMw-HA. Therefore, our observations may have important implications for the development of future drug delivery systems (DDS) as LMw-HA bearing NPs may safely replace polyethylene glycol (PEG) when passive delivery is required, since complement activation can be by-passed. Finally, HMw-HA NPs could be used for active targeting of CD44 overexpressing tumors and aberrantly activated leukocytes in inflammation.

#### Acknowledgements

S.M. thanks TAU Nano Center for Ph.D. fellowship. SMM gratefully acknowledges financial support by the Danish Agency for Science, Technology and Innovation reference 09-065746/DSF. This work was supported in part by grants from the Alon Foundation, the Marie Curie IRG-FP7 of the European Union, Levy Family Trust and Israel Science Foundation (Award #181/10), and the I-core excellence center on human complex diseases to DP.

#### References

- [1] A. Varki, Essentials of glycobiology, Cold Spring Harbor Laboratory Press, Cold Spring Harbor, N.Y., 2009
- [2] B.P. Toole, Hyaluronan: from extracellular glue to pericellular cue, *Nat. Rev. Cancer* 4 (7) (2004) 528–539.
- [3] V.M. Platt, F.C. Szoka Jr., Anticancer therapeutics: targeting macromolecules and nanocarriers to hyaluronan or CD44, a hyaluronan receptor, *Mol. Pharm.* 5 (4) (2008) 474–486.
- [4] T. Pouyani, G.D. Prestwich, Functionalized derivatives of hyaluronic acid oligosaccharides: drug carriers and novel biomaterials, *Bioconjug. Chem.* 5 (4) (1994) 339–347.
- [5] G.D. Prestwich, D.M. Marecak, J.F. Marecek, K.P. Verduyse, M.R. Ziebell, Controlled chemical modification of hyaluronic acid: synthesis, applications, and biodegradation of hydrazide derivatives, *J. Control. Release* 53 (1–3) (1998) 93–103.
- [6] R.E. Eliaz, S. Nir, F.C. Szoka Jr., Interactions of hyaluronan-targeted liposomes with cultured cells: modeling of binding and endocytosis, *Methods Enzymol.* 387 (2004) 16–33.
- [7] R.E. Eliaz, F.C. Szoka Jr., Liposome-encapsulated doxorubicin targeted to CD44: a strategy to kill CD44-overexpressing tumor cells, *Cancer Res.* 61 (6) (2001) 2592–2601.
- [8] D. Peer, A. Florentin, R. Margalit, Hyaluronan is a key component in cryoprotection and formulation of targeted unilamellar liposomes, *Biochim. Biophys. Acta* 1612 (1) (2003) 76–82.
- [9] D. Peer, R. Margalit, Tumor-targeted hyaluronan nanoliposomes increase the antitumor activity of liposomal Doxorubicin in syngeneic and human xenograft mouse tumor models, *Neoplasia* 6 (4) (2004) 343–353.
- [10] D. Peer, R. Margalit, Loading mitomycin C inside long circulating hyaluronan targeted nano-liposomes increases its antitumor activity in three mice tumor models, *Int. J. Cancer* 108 (5) (2004) 780–789.
- [11] D. Peer, E.J. Park, Y. Morishita, C.V. Carman, M. Shimaoka, Systemic leukocyte-directed siRNA delivery revealing cyclin D1 as an anti-inflammatory target, *Science* 319 (5863) (2008) 627–630.
- [12] I. Rivkin, K. Cohen, J. Koffler, D. Melikhov, D. Peer, R. Margalit, Paclitaxel-clusters coated with hyaluronan as selective tumor-targeted nanovectors, *Biomaterials* 31 (27) (2010) 7106–7114.
- [13] K.K. Upadhyay, A.N. Bhatt, A.K. Mishra, B.S. Dwarakanath, S. Jain, C. Schatz, J.F. Le Meins, A. Farooque, G. Chandraiah, A.K. Jain, A. Misra, S. Lecommandoux, The intracellular drug delivery and anti tumor activity of doxorubicin loaded poly( $\gamma$ -benzyl L-glutamate)-b-hyaluronan polymersomes, *Biomaterials* 31 (10) (2010) 2882–2892.
- [14] K.K. Upadhyay, A.N. Bhatt, E. Castro, A.K. Mishra, K. Chuttani, B.S. Dwarakanath, C. Schatz, J.F. Le Meins, A. Misra, S. Lecommandoux, In vitro and in vivo evaluation of docetaxel loaded biodegradable polymersomes, *Macromol. Biosci.* 10 (5) (2010) 503–512.
- [15] S. Mohapatra, X. Yang, J.A. Wright, E.A. Turley, A.H. Greenberg, Soluble hyaluronan receptor RHAMM induces mitotic arrest by suppressing Cdc2 and cyclin B1 expression, *J. Exp. Med.* 183 (4) (1996) 1663–1668.
- [16] A.J. Day, G.D. Prestwich, Hyaluronan-binding proteins: tying up the giant, *J. Biol. Chem.* 277 (7) (2002) 4585–4588.
- [17] H. Shigeishi, S. Fujimoto, M. Hiraoka, S. Ono, M. Taki, K. Ohta, K. Higashikawa, N. Kamata, Overexpression of the receptor for hyaluronan-mediated motility, correlates with expression of microtubule-associated protein in human oral squamous cell carcinomas, *Int. J. Oncol.* 34 (6) (2009) 1565–1571.
- [18] D.S. Krause, T.R. Spitzer, C.P. Stowell, The concentration of CD44 is increased in hematopoietic stem cell grafts of patients with acute myeloid leukemia, plasma cell myeloma, and non-Hodgkin lymphoma, *Arch. Pathol. Lab. Med.* 134 (7) (2010) 1033–1038.
- [19] R. Stern, A.A. Asari, K.N. Sugahara, Hyaluronan fragments: an information-rich system, *Eur. J. Cell Biol.* 85 (8) (2006) 699–715.
- [20] R. Kedmi, N. Ben-Arie, D. Peer, The systemic toxicity of positively charged lipid nanoparticles and the role of Toll-like receptor 4 in immune activation, *Biomaterials* 31 (26) (2010) 6867–6875.
- [21] D. Peer, R. Margalit, Physicochemical evaluation of a stability-driven approach to drug entrapment in regular and in surface-modified liposomes, *Arch. Biochem. Biophys.* 383 (2) (2000) 185–190.
- [22] B. Johnsson, S. Lofas, G. Lindquist, Immobilization of proteins to a carboxymethyl-dextran-modified gold surface for biospecific interaction analysis in surface plasmon resonance sensors, *Anal. Biochem.* 198 (2) (1991) 268–277.
- [23] D.G. Myszka, Improving biosensor analysis, *J. Mol. Recognit.* 12 (5) (1999) 279–284.
- [24] D.G. Myszka, T.A. Morton, CLAMP: a biosensor kinetic data analysis program, *Trends Biochem. Sci.* 23 (4) (1998) 149–150.
- [25] D. Peer, Y. Dekel, D. Melikhov, R. Margalit, Fluoxetine inhibits multidrug resistance extrusion pumps and enhances responses to chemotherapy in syngeneic and in human xenograft mouse tumor models, *Cancer Res.* 64 (20) (2004) 7562–7569.
- [26] I. Hamad, A.C. Hunter, J. Szebeni, S.M. Moghimi, Poly(ethylene glycol)s generate complement activation products in human serum through increased alternative pathway turnover and a MASP-2-dependent process, *Mol. Immunol.* 46 (2) (2008) 225–232.
- [27] S.M. Moghimi, I. Hamad, T.L. Andresen, K. Jorgensen, J. Szebeni, Methylation of the phosphate oxygen moiety of phospholipid-methoxy(polyethylene glycol) conjugate prevents PEGylated liposome-mediated complement activation and anaphylatoxin production, *FASEB J.* 20 (14) (2006) 2591–2593.
- [28] I. Hamad, O. Al-Hanbali, A.C. Hunter, K.J. Rutt, T.L. Andresen, S.M. Moghimi, Distinct polymer architecture mediates switching of complement activation pathways at the nanosphere-serum interface: implications for stealth nanoparticle engineering, *ACS Nano* 4 (11) (2010) 6629–6638.
- [29] Y.S. Day, C.L. Baird, R.L. Rich, D.G. Myszka, Direct comparison of binding equilibrium, thermodynamic, and rate constants determined by surface- and solution-based biophysical methods, *Protein Sci.* 11 (5) (2002) 1017–1025.
- [30] D. Wild, The Immunoassay handbook, Nature Pub Group, London, 2001.
- [31] P.M. Wolny, S. Banerji, C. Gounou, A.R. Brisson, A.J. Day, D.G. Jackson, R.P. Richter, Analysis of CD44-hyaluronan interactions in an artificial membrane system: insights into the distinct binding properties of high and low molecular weight hyaluronan, *J. Biol. Chem.* 285 (39) (2010) 30170–30180.
- [32] S. Ogino, N. Nishida, R. Umemoto, M. Suzuki, M. Takeda, H. Terasawa, J. Kitayama, M. Matsumoto, H. Hayasaka, M. Miyasaka, I. Shimada, Two-state conformations in the hyaluronan-binding domain regulate CD44 adhesiveness under flow condition, *Structure* 18 (5) (2010) 649–656.
- [33] J. Lesley, V.C. Hascall, M. Tammi, R. Hyman, Hyaluronan binding by cell surface CD44, *J. Biol. Chem.* 275 (35) (2000) 26967–26975.
- [34] T.C. Laurent, J.R. Fraser, H. Perftoft, B. Smedsrud, Binding of hyaluronate and chondroitin sulphate to liver endothelial cells, *Biochem. J.* 234 (3) (1986) 653–658.
- [35] A. Visintin, A. Mazzoni, J.H. Spitzer, D.H. Wyllie, S.K. Dower, D.M. Segal, Regulation of Toll-like receptors in human monocytes and dendritic cells, *J. Immunol.* 166 (1) (2001) 249–255.
- [36] C.S. Alves, M.M. Burdick, S.N. Thomas, P. Pawar, K. Konstantopoulos, The dual role of CD44 as a functional P-selectin ligand and fibrin receptor in colon carcinoma cell adhesion, *Am. J. Physiol. Cell Physiol.* 294 (4) (2008) C907–916.
- [37] S. Banerji, B.R.S. Hide, J.R. James, M.E.M. Noble, D.G. Jackson, Distinctive Properties of the Hyaluronan-binding Domain in the Lymphatic Endothelial Receptor Lyve-1 and Their Implications for Receptor Function, *J. Biol. Chem.* 285 (14) (2010) 10724–10735.
- [38] L.E. Sebban, D. Ronen, D. Levartovsky, O. Elkayam, D. Caspi, S. Aamar, H. Amital, A. Rubinow, I. Golan, D. Naor, Y. Zick, I. Golan, The involvement of CD44 and its novel ligand galectin-8 in apoptotic regulation of autoimmune inflammation, *J. Immunol.* 179 (2) (2007) 1225–1235.
- [39] C.A. Cuff, D. Kothapalli, I. Azonobi, S. Chun, Y. Zhang, R. Belkin, C. Yeh, A. Secretro, R.K. Assoian, D.J. Rader, E. Pure, The adhesion receptor CD44 promotes atherosclerosis by mediating inflammatory cell recruitment and vascular cell activation, *J. Clin. Invest.* 108 (7) (2001) 1031–1040.
- [40] D. Kothapalli, J. Flowers, T. Xu, E. Pure, R.K. Assoian, Differential activation of ERK and Rac mediates the proliferative and anti-proliferative effects of hyaluronan and CD44, *J. Biol. Chem.* 283 (46) (2008) 31823–31829.
- [41] D. Kothapalli, L. Zhao, E.A. Hawthorne, Y. Cheng, E. Lee, E. Pure, R.K. Assoian, Hyaluronan and CD44 antagonize mitogen-dependent cyclin D1 expression in mesenchymal cells, *J. Cell Biol.* 176 (4) (2007) 535–544.

- [42] D.C. West, S. Kumar, The effect of hyaluronate and its oligosaccharides on endothelial cell proliferation and monolayer integrity, *Exp. Cell Res.* 183 (1) (1989) 179–196.
- [43] T. Ahrens, V. Assmann, C. Fieber, C. Termeer, P. Herrlich, M. Hofmann, J.C. Simon, CD44 is the principal mediator of hyaluronic-acid-induced melanoma cell proliferation, *J. Invest. Dermatol.* 116 (1) (2001) 93–101.
- [44] K.A. Scheibner, M.A. Lutz, S. Boodoo, M.J. Fenton, J.D. Powell, M.R. Horton, Hyaluronan fragments act as an endogenous danger signal by engaging TLR2, *J. Immunol.* 177 (2) (2006) 1272–1281.
- [45] D. Jiang, J. Liang, J. Fan, S. Yu, S. Chen, Y. Luo, G.D. Prestwich, M.M. Mascarenhas, H.G. Garg, D.A. Quinn, R.J. Homer, D.R. Goldstein, R. Bucala, P.J. Lee, R. Medzhitov, P.W. Noble, Regulation of lung injury and repair by Toll-like receptors and hyaluronan, *Nat. Med.* 11 (11) (2005) 1173–1179.
- [46] M.R. Horton, M.D. Burdick, R.M. Strieter, C. Bao, P.W. Noble, Regulation of hyaluronan-induced chemokine gene expression by IL-10 and IFN-gamma in mouse macrophages, *J. Immunol.* 160 (6) (1998) 3023–3030.
- [47] M.J. Wang, J.S. Kuo, W.W. Lee, H.Y. Huang, W.F. Chen, S.Z. Lin, Translational event mediates differential production of tumor necrosis factor-alpha in hyaluronan-stimulated microglia and macrophages, *J. Neurochem.* 97 (3) (2006) 857–871.
- [48] D. Krejcova, M. Pekarova, B. Safrankova, L. Kubala, The effect of different molecular weight hyaluronan on macrophage physiology, *Neuro Endocrinol. Lett.* 30 (Suppl 1) (2009) 106–111.
- [49] C.M. McKee, M.B. Penno, M. Cowman, M.D. Burdick, R.M. Strieter, C. Bao, P.W. Noble, Hyaluronan (HA) fragments induce chemokine gene expression in alveolar macrophages. The role of HA size and CD44, *J. Clin. Invest.* 98 (10) (1996) 2403–2413.
- [50] C.R. Amura, T. Kamei, N. Ito, M.J. Soares, D.C. Morrison, Differential regulation of lipopolysaccharide (LPS) activation pathways in mouse macrophages by LPS-binding proteins, *J. Immunol.* 161 (5) (1998) 2552–2560.
- [51] B. Beutler, Inferences, questions and possibilities in Toll-like receptor signalling, *Nature* 430 (6996) (2004) 257–263.
- [52] D.F. Fiorentino, A. Zlotnik, T.R. Mosmann, M. Howard, A. O'Garra, IL-10 inhibits cytokine production by activated macrophages, *J. Immunol.* 147 (11) (1991) 3815–3822.
- [53] A. Chanan-Khan, J. Szebeni, S. Savay, L. Liebes, N.M. Rafique, C.R. Alving, F.M. Muggia, Complement activation following first exposure to pegylated liposomal doxorubicin (Doxil): possible role in hypersensitivity reactions, *Ann. Oncol.* 14 (9) (2003) 1430–1437.
- [54] R. Gorodetsky, L. Levdansky, A. Vexler, I. Shimeliovich, I. Kassis, M. Ben-Moshe, S. Magdassi, G. Marx, Liposome transduction into cells enhanced by haptotactic peptides (Haptides) homologous to fibrinogen C-termini, *J. Control. Release* 95 (3) (2004) 477–488.
- [55] S.M. Moghimi, J. Szebeni, Stealth liposomes and long circulating nanoparticles: critical issues in pharmacokinetics, opsonization and protein-binding properties, *Prog. Lipid Res.* 42 (6) (2003) 463–478.
- [56] J. Szebeni, L. Baranyi, S. Savay, H.U. Lutz, E. Jelezarova, R. Bunger, C.R. Alving, The role of complement activation in hypersensitivity to pegylated liposomal doxorubicin (DOXIL (R)), *J. Liposome Res.* 10 (4) (2000) 467–481.